



Influence of erythrocyte aggregation on radial migration of platelet-sized spherical particles in shear flow



Cyrille Guilbert^{a,1}, Boris Chayer^a, Louise Allard^a, François T.H. Yu^{a,2}, Guy Cloutier^{a,b,c,*}

^aLaboratory of Biorheology and Medical Ultrasonics, University of Montreal Hospital Research Center (CRCHUM), Montréal, Québec, Canada

^bInstitute of Biomedical Engineering, University of Montreal, Montréal, Québec, Canada

^cDepartment of Radiology, Radio-oncology and Nuclear Medicine, University of Montreal, Montréal, Québec, Canada

ARTICLE INFO

Article history:
Accepted 29 June 2017

Keywords:
Mimicking platelets
Red blood cell aggregation
Cell migration
Biorheology
Micro particle dynamics
Couette flow experiments

ABSTRACT

Blood platelets when activated are involved in the mechanisms of hemostasis and thrombosis, and their migration toward injured vascular endothelium necessitates interaction with red blood cells (RBCs). Rheology co-factors such as a high hematocrit and a high shear rate are known to promote platelet mass transport toward the vessel wall. Hemodynamic conditions promoting RBC aggregation may also favor platelet migration, particularly in the venous system at low shear rates. The aim of this study was to confirm experimentally the impact of RBC aggregation on platelet-sized micro particle migration in a Couette flow apparatus. Biotin coated micro particles were mixed with saline or blood with different aggregation tendencies, at two shear rates of 2 and 10 s⁻¹ and three hematocrits ranging from 20 to 60%. Streptavidin membranes were respectively positioned on the Couette static and rotating cylinders upon which the number of adhered fluorescent particles was quantified. The platelet-sized particle adhesion on both walls was progressively enhanced by increasing the hematocrit ($p < 0.001$), reducing the shear rate ($p < 0.001$), and rising the aggregation of RBCs ($p < 0.001$). Particle count was minimum on the stationary cylinder when suspended in saline at 2 s⁻¹ (57 ± 33), and maximum on the rotating cylinder at 60% hematocrit, 2 s⁻¹ and the maximum dextran-induced RBC aggregation (2840 ± 152). This fundamental study is confirming recent hypotheses on the role of RBC aggregation on venous thrombosis, and may guide molecular imaging protocols requiring injecting active labeled micro particles in the venous flow system to probe human diseases.

© 2017 Elsevier Ltd. All rights reserved.

1. Introduction

Platelets play major roles in multiple mechanisms of hemostasis and thrombotic events. They intervene in repairing vascular injury to prevent further blood lost or pathologically to induce thrombus growth. Therefore, platelets must leave the main blood stream and adhere to the vascular endothelium of damaged or inflamed sites. Red blood cells (RBCs), because of their size, their aptitude to deform as well as their important volume fraction in blood, facilitate transport of platelets within blood vessels (Aarts et al., 1983, 1984; Eckstein et al., 1988; Turitto and Hall, 1998; Zhao et al., 2012; Reasor et al., 2013; Litvinov and Weisel, 2017).

A contemporary review of blood margination (*i.e.*, radial displacement of leukocytes and platelets toward the wall) and segregation (*i.e.*, spatial redistribution of blood elements) phenomena can be found in Kumar and Graham (2012).

1.1. Mass transport

Transport of matter in a fluid can be done by convection (due to the principal flux) and/or diffusion (due to chaotic movement). *In vitro*, adhesion of platelets to the vascular wall was almost abolished in the absence of human RBCs because platelets travelled parallel to streamlines due to convection only (Aarts et al., 1983). Similar behavior was observed *in vivo*, the presence of RBCs had a strong impact on micro particle margination in microvessels (D'Apolito et al., 2015). The presence of RBCs would promote particle diffusion through a *turbulent mixing effect* (Keller, 1971). Deformable particles, such as RBCs in shear flow, exhibit a steady stationary-orientation motion or an unsteady flipping motion (Keller and Skalak, 1982; Barthes-Biesel and Sgaier, 1985) that

* Corresponding author at: Laboratory of Biorheology and Medical Ultrasonics, University of Montreal Hospital Research Center (CRCHUM), Montréal, Québec, Canada.

E-mail address: guy.cloutier@umontreal.ca (G. Cloutier).

¹ Now with the Centre Hospitalier de la Côte Basque (CHCB), Bayonne, France.

² Now with the Center for Ultrasound Molecular Imaging and Therapeutics, University of Pittsburgh, Pittsburgh, Pennsylvania, USA.

contribute to platelet margination. RBCs migrate toward the center of blood vessels and their deformability expulses the smaller platelets from the central flow toward the vessel wall. Through this mechanism, a two-phase region is anticipated: a region rich in RBCs and poor in platelets at the vessel center, and a region rich in platelets and poor in RBCs at the periphery. Diffusive transport is provoked by the constant collisions of suspended particles. Since there are more particles per unit volume in the central region of a blood vessel, platelets tend to migrate from the interior of the vessel to the vascular wall, as observed experimentally by laser Doppler (Aarts et al., 1988).

The rotation of RBCs in shear flow has a *swept-out volume* whose amplitude depends on the RBC deformability (Chien, 1975). The more the RBC deforms, the less the swept out volume is important. Goldsmith (1972) proposed that RBCs undergo an erratic radial displacement resulting from constant collisions between suspended particles, thus provoking the radial diffusion of platelets. With this theory, the rate at which platelets are transported is proportional to the shear rate and the hematocrit but not to the diameter of the RBC. The enhancement of micro particle migration with shear rate was experimentally observed in a microfluidics system at shear rates between 800 and 2500 s⁻¹, when interacting with 10% hematocrit RBCs (D'Apolito et al., 2016). The presence of a *skimming layer* (Aarts et al., 1983) could constitute another explanation for the platelet diffusion phenomenon. This effect is attributed to the important size difference between RBCs and platelets. Interestingly, both theories lead to the same conclusion that RBCs favor platelet migration toward the vessel wall.

1.2. Effect of RBC volume concentration

The presence of RBCs at 40–50% hematocrit considerably contributes to the displacement of platelets and leukocytes, and their adhesion on the endothelium surface (Goldsmith et al., 1999). At such a high volume concentration, one might think that RBCs would limit the diffusion of suspended particles. This is only true under plug flow when moving blood is stationary with no streamline mixing (Goldsmith and Turitto, 1986). At the opposite, the presence of a velocity gradient promotes collisions of cells approaching on adjacent streamlines. By observing the movement of tracer particles in a suspension of transparent ghost RBCs (*i.e.*, hemoglobin-less RBCs) under laminar flow using a travelling microscope, several findings on cell kinetics have been reported (Goldsmith, 1993): (1) In the absence of ghost erythrocytes, tracer particles travelled undisturbed and parallel to the vascular wall; (2) when ghost RBCs were added, cellular collisions increased and a random lateral displacement of smaller spherical tracer particles was noticed (Goldsmith and Marlow, 1979); and (3) collisions with the vascular wall occurred and the frequency of collision increased with the ghost RBC volume concentration. Recent simulations of microcirculatory flow at 24% hematocrit also reported that the frequency of collisions with RBCs favors micro particle margination (Vahidkhah and Bagchi, 2015).

1.3. Influence of RBC aggregation

Inflammatory conditions promote abnormal RBC hyper-aggregation (Weng et al., 1996a, 1998; Ben Ami et al., 2001; Berliner et al., 2005; Maharskak et al., 2009; Reggiori et al., 2009; Tripette et al., 2013). The hyperviscosity provoked by this phenomenon increases the interaction time of platelets with the vascular wall and favors venous thrombotic events (Yu et al., 2011). However, the decisive role of RBC aggregation on platelet radial migration is still underexplored. Nash et al. (2008) proposed that even though RBC aggregation is not required for the margination of platelets, its presence would favor it. Opposite results were,

however, obtained *in vivo* using the intravital microscopy technique and fluorescently labeled platelets flowing in rabbit mesenteric arterioles and venules. RBC hyper-aggregation induced by high-molecular weight dextran infusion reduced the platelet count at the wall (Woldhuis et al., 1993). Using the same technique, RBC aggregation promoted leukocyte margination in rat postcapillary venules and their adhesion on the endothelium (Pearson and Lipowsky, 2000). The enhancement of leukocyte margination with RBC aggregation has also been demonstrated in a rectangular channel microfluidic system (Jain and Munn, 2009).

1.4. Objective

The current study aimed to quantify experimentally in a Couette flow device the radial migration of platelet-sized micro particles as a function of RBC aggregation, flow shear rate and blood hematocrit. RBC aggregation is a recognized thrombotic co-factor (Mackman, 2012) that has been postulated to trigger venous thrombosis (Yu et al., 2011). The current study proves the direct impact of RBC aggregation on mimicking platelet transport, which is required for interaction with the vessel wall during venous thrombosis. This work may also shed some light and guide molecular imaging protocols based on the injection of micro particles into the venous system (Kato et al., 2009). Experimental data are also required to better understand the interaction of drug micro carriers with blood flow properties (Müller et al., 2014), and the current study may provide new evidences.

2. Materials and methods

2.1. Experimental considerations

Platelets play an important role in the mechanisms of thrombosis and hemostatic plug despite the fact that they occupy only ~0.7% of the blood cellular phase volume. This is due to their very strong reactivity once activated. Platelets manipulated outside the human body coagulate very quickly on synthetic surfaces. It is therefore very difficult to work with blood platelets without anticoagulation (Schneider et al., 1997). However, anticoagulation inhibits adenosine diphosphate induced platelet activation and, therefore, platelet adhesion. Thus, a protocol aiming at determining the impact of RBC aggregation on platelet interaction with a vessel wall would be difficult with native anticoagulated platelets. Because this study does not address the biology but the rheology of blood platelets, we propose to replace them with micro particles that have similar physical dimensions and controllable adhesion properties. Since physiological flow in blood vessels implies a spatial variation of the shear rate contributing to the micro particle margination process, we opted instead for a Couette flow system with an aspect ratio providing a close to constant shear rate in the gap between rotating cylinders (Whorlow, 1980). With such device, the confounding impact of the radial shear rate gradient on RBC aggregation did not have to be considered when interpreting our results.

2.2. Preparation of blood samples

Fresh porcine whole blood, anticoagulated with 3 g/L of ethylene diamine tetra acetic acid (EDTA ACS reagent, 99.4%, Sigma Chemical, St. Louis, MO, USA), was obtained from a local slaughter house. The buffy coat was removed after a first centrifugation at 2500 rotations per minute during 15 min. The plasma was separated from the RBCs and replaced with an isotonic saline solution for a second centrifugation. The saline suspension was aspirated to remove residual platelets and white blood cells. RBCs were resuspended in native plasma or in a saline solution.

Nine blood aliquots of 70 mL were prepared from every porcine blood sample by adjusting the hematocrit to 20%, 40% and 60%, and the RBC aggregation level into 3 categories: no aggregation (NA), normal aggregation (A) and hyper-aggregation (HA). NA samples were obtained by suspending RBCs into physiological isotonic saline. Normal A samples were obtained by reconstituting RBCs with the native plasma (porcine RBCs have a similar aggregation tendency as human RBCs (Weng et al., 1996b)). HA samples were prepared by mixing RBCs with a dextran solution. Dextran powder (512 kDa, D5251, lot 124H0055, Sigma Chemical, St. Louis, MO, USA) was dissolved into isotonic saline at a concentration of 30 g/L (Boynard and Lelievre, 1990; Neu and Meiselman, 2002). Five experimental series were realized for every blood sample at a given shear rate and hematocrit. All experiments were conducted within 48 h after blood collection. Two control solutions (no RBCs) were tested to verify the degree of micro particle migration in the absence of erythro-

cytes: an isotonic saline solution was used as controls for NA and A blood samples, whereas an isotonic saline mixed with dextran 512 (30 g/L) was chosen to compare results with HA blood solution experiments.

2.3. Platelet mimicking particles

Biotin coated fluorescent spherical micro particles (Bangs Laboratories, Fishers, IN) were used as platelet phantoms. The micro particle diameter and density (2 μm and 1.06 g/mL) were about the same as blood platelets (2 μm and 1.062 g/mL (Savage et al., 1986)). The micro particle volume solution to use for each experiment was determined empirically (300 μL with 1% solid particles). It was chosen by considering the strongest obtainable fluorescent intensity while maintaining a linear response for quantification (Amersham Biosciences, 2008). Considering that there are 150–400 $\times 10^3$ platelets/ μL of human blood, therefore for 70 mL of blood used for each experiment, the estimated number of micro particles to be used for replacing platelets was between $1\text{--}3 \times 10^{10}$ (we had 7×10^{11} micro particles into 300 μL of solution, which is higher but comparable). To mimic the endothelium attractive property, a biotin-capture SAM2 membrane (model V2861, Promega, Madison, WI) was used to bind flowing biotinylated micro particles. These membranes came partially cut allowing an easy separation into 96 individual squares. They were designed for small-scale experiments where high binding capacity is required (Promega, 2008).

2.4. Experimental setup

The Couette flow apparatus (Fig. 1) was designed and manufactured by our group for blood rheological experiments (Yu et al., 2009). The blood sample was introduced within a 2-mm annulus between two concentric cylinders of radii $R_1 = 80$ mm and $R_2 = 82$ mm. The external cylinder is fixed and the inner cylinder is driven by a step motor and a motor driver (Parker Compumotor, models LN57-170 and Zeta6104, Richmond, CA) at a constant clockwise angular velocity. For $(R_2 - R_1)/R_1 \ll 1$, then the shear rate $\dot{\gamma}$ in s^{-1} is given by Whorlow (1980):

$$\dot{\gamma} = \frac{4\pi \times R_1 \times R_2}{R_2^2 - R_1^2} \times v = 154 \times v \quad (1)$$

where v is the rotation speed in revolution per second.

As seen in Fig. 1, the Couette device possesses an opening on the external cylinder, 3.5 cm from its base, to allow micro particle solution injection via a 3 cm^3 syringe, a 70 mm long needle and a syringe pump (PHD 2000, Harvard apparatus, Holliston, MA). The 300 μL micro particle solution was mixed with 1 mL of blood using a vortex mixer prior to pipetting. The entire apparatus was maintained at room temperature.

2.5. Biotin-capturing membrane positioning

One membrane of 1 by 1 cm^2 was fixed on each internal wall of the Couette apparatus. The back of each membrane was gently covered with a commercial adhesive spray (Nashua covalent adhesives 357) and fixed 3–3.5 cm from the base

of the wall (far enough to avoid hematocrit variations in case of improbable sedimentation). The membrane fixed on the rotating cylinder was positioned on the left of the needle, whereas the one on the stationary cylinder was fixed to the right of the needle. This way the membranes did not come in contact with microspheres during injection.

2.6. Measuring protocol

The first part of the study consisted in varying the hematocrit as well as the aggregation level of RBCs at a constant shear rate of 2 s^{-1} . In the second part, the RBC aggregation was varied and the hematocrit was fixed to 40% at a constant shear rate of 10 s^{-1} . Prior to measurements, the blood sample was sheared at 500 s^{-1} for 30 s to break-up all aggregates and to mix blood. The shear rate was then reduced to the targeted value for 70 s to wait for the aggregation kinetics to stabilize. After that, the Couette apparatus performed three complete revolutions. During the first revolution, the injection of micro particles was performed at a rate of 0.6 mL/min (for the shear rate of 2 s^{-1}) or 3 mL/min (for 10 s^{-1}) to ensure a homogeneous distribution. At the end of the first revolution, the needle was removed from the annulus to prevent any flow disturbance. The binding of migrating micro particles was allowed for the remaining two revolutions. At the end of the third revolution, the rotating cylinder was automatically lifted up to avoid any further contact between both membranes and flowing microspheres. Three revolutions were selected to avoid recirculation of injected micro particles and any further contact with streptavidin membranes. Selected shear rates of 2 s^{-1} and 10 s^{-1} are typical of venous flow conditions (Fung, 1997).

2.7. Quantification of particle counts on both membranes

Once each experiment was completed, the membranes were gently detached from the Couette annulus with forceps and inserted in a washing solution. All non-specific adhesive molecules on both membranes were removed following a 20 min washing protocol (Schaefer and Guimond, 1998). Using an oscillating shaker (model G2, Gyrotory, Eppendorf Inc., Hamburg, Germany), each membrane was then cleaned during 30 s with 200 mL of 2 M NaCl (product #8B6796, Bioshop Canada Inc., Burlington, ON), 3 times during 120 s with another 200 mL of 2 M NaCl, 4 times during 120 s with 200 mL of 2 M NaCl with 1% H₃PO₄ (H₃PO₄ ≥ 85 WT% solution in water reagent, product #438001-500 mL, Sigma-Aldrich, Saint-Louis, MO), 2 times during 30 s with 100 mL of demonized water and 10 s with 95% ethanol (this last step is accelerating the drying stage and is optional). The membranes were then maintained between 2 and 8 $^\circ\text{C}$ (Promega, 2008).

Membranes were then scanned using a Typhoon PhosphorImager (Typhoon 8600 Variable Mode Imager, Molecular Dynamics, Sunnyvale, CA) (McNamara et al., 2001). The maximum spatial resolution of the Typhoon laser was set to 25 μm (the maximum particle count for 1 by 1 cm membranes was 160,000). The focal plane parameter was set to Platern + press sample, the sensitivity was normal and the photomultiplier voltage was set to 430 V. Scans were quantified with ImageQuant 2005 software (Amersham Biosciences, 2008) using the colony count feature with an operator size of 7.

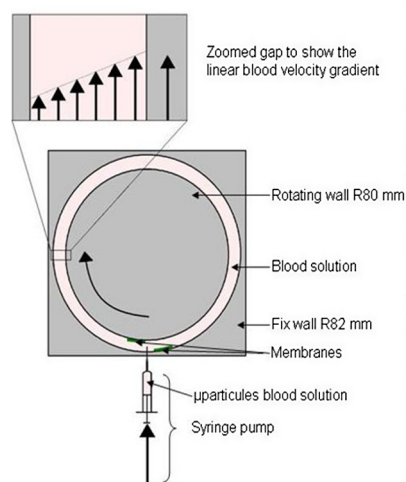


Fig. 1. Experimental Couette flow device (schematic view on the left, picture on the right).

2.8. Statistical analysis

Three way analyses of variance with Tukey test (SigmatStat 3.11, Systat software, San Jose, CA) were performed to evaluate the effect of the hematocrit, shear rate and RBC aggregation level on the migration of micro particles. Otherwise specified, $p < 0.001$ was considered as statistically significant (Johnson, 2013).

3. Results

Fig. 2 shows examples of fluorescent particle counts obtained for different micro particle migrations. As presented in Tables 1 and 2, the number of micro particles counted on rotating membranes was always superior to that measured on fixed membranes ($p < 0.033$). This was verified for all saline and blood solutions. The number of adhesive micro particles was smaller when using a saline suspension compared with blood experiments at both shear rates (Table 2). For convenience, only results for rotating membranes are given in the remaining of this manuscript (conclusions are the same for particle counts measured on stationary membranes).

3.1. Micro particle count for different RBC aggregation levels and hematocrits at a shear rate of 2 s^{-1}

As illustrated in Fig. 3, the number of migrating micro particles attached to the rotating Couette wall increased significantly with the hematocrit ($p < 0.001$) and the aggregation property of RBCs ($p < 0.001$). The smallest count was obtained with the control sal-

ine suspension (0% hematocrit). Pairwise comparisons (Tukey post hoc test) showed no difference between the saline suspension (no RBCs) and saline suspension of RBCs at 20% hematocrit. All other pairwise differences were statistically significant ($p < 0.001$).

3.2. Micro particle count for different RBC aggregation levels and two shear rates at a hematocrit of 40%

The number of counted micro particles was minimum in saline and increased with RBC aggregation ($p < 0.001$) or a reduction of the shear rate ($p < 0.001$, Fig. 4). Statistically significant pairwise differences (Tukey test) are illustrated on the figure.

4. Discussion

In flow conditions inhibiting RBC aggregation, causes of platelet margination are related to blood hematocrit (Goldsmith and Turitto, 1986; Cadroy and Hanson, 1990; Eugster and Reinhart, 2005; Almomani et al., 2008), flow shear rate (Goldsmith, 1972), RBC dimension (Aarts et al., 1983) and RBC deformability (Aarts et al., 1984), affecting erratic radial displacement and interactions with platelets. Only a few studies have looked at RBC aggregation as a potential cause of platelet or leukocyte margination (Woldhuis et al., 1993; Goldsmith et al., 1999; Jain and Munn, 2009). Although contradictory, these results suggest a non-negligible effect of RBC aggregation on micro particle migration toward the vessel wall.

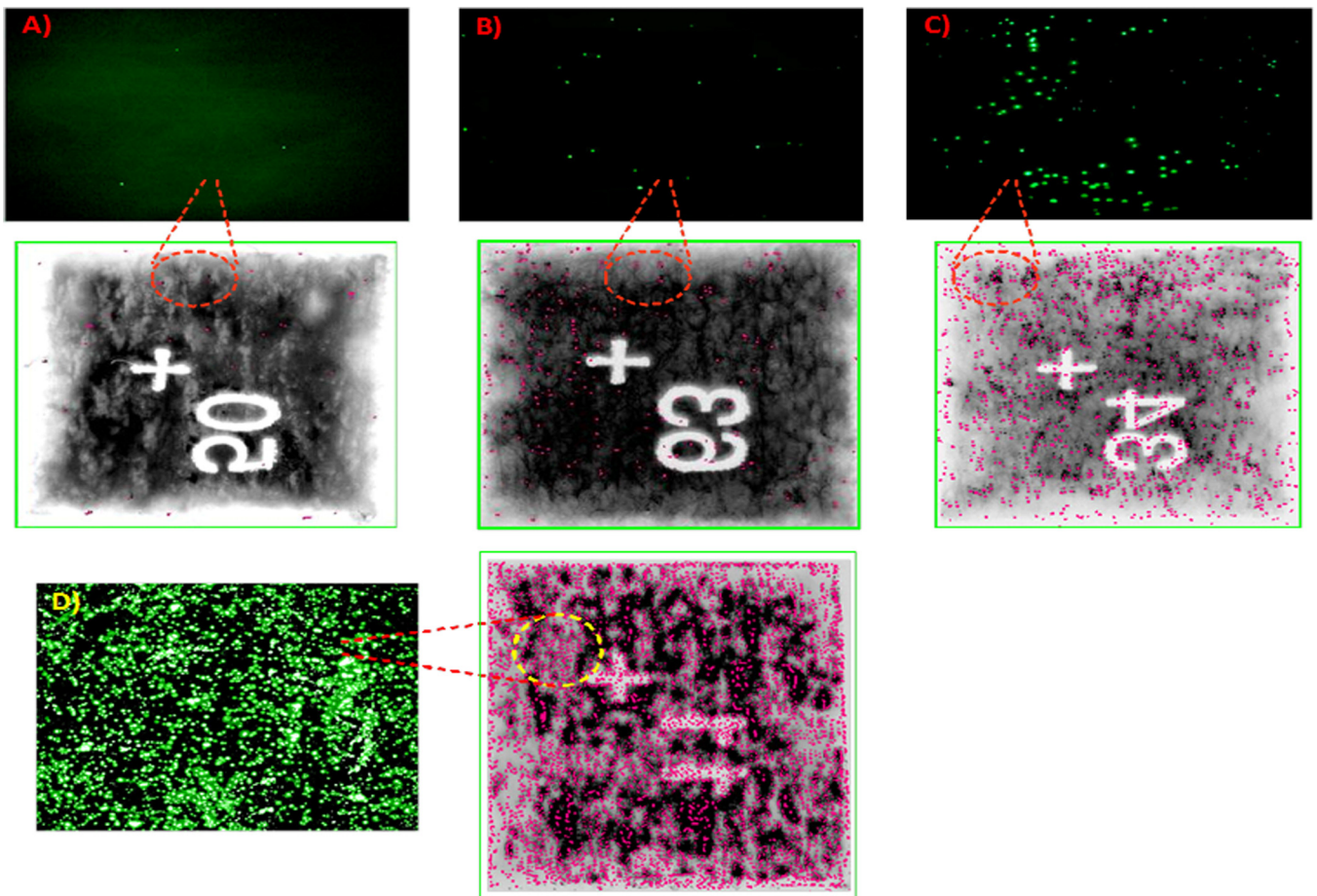


Fig. 2. Microscopic observation ($10\times$) of the biotin-capturing membranes for (A) a low fluorescent particle count between 0 and 200, (B) a count between 200 and 1000, (C) a count >1000 , and (D) a count >2000 . The zoomed sections on A-D correspond to the automatic particle counts obtained with the Typhoon PhosphorImager. They were 28 (A), 220 (B), 1269 (C) and 2979 (D) for these examples. The membrane number for identification was always visible.

Table 1

Mean \pm standard deviation of the number of micro particles captured by the rotating and stationary SAM2 membranes fixed on the Couette flow cylinders for non-aggregating (NA), normal aggregating (A) and hyper-aggregating (HA) red blood cells at 20% (H20), 40% (H40) and 60% (H60) hematocrits. The shear rate was 2 s^{-1} for all measurements. For comparison, the number of micro particles on the rotating membrane when filling the gap of both concentric cylinders with saline was 80 ± 32 , whereas it was 57 ± 33 on the stationary membrane. The use of saline prevented interactions of micro particles with red blood cells.

| | H20 2 s^{-1} | | H40 2 s^{-1} | | H60 2 s^{-1} | |
|----|------------------------|---------------|------------------------|---------------|------------------------|----------------|
| | Rotating | Stationary | Rotating | Stationary | Rotating | Stationary |
| NA | 151 \pm 34 | 70 \pm 34 | 566 \pm 53 | 244 \pm 200 | 1289 \pm 117 | 941 \pm 159 |
| A | 424 \pm 55 | 196 \pm 47 | 1077 \pm 230 | 604 \pm 100 | 1695 \pm 86 | 1024 \pm 278 |
| HA | 579 \pm 140 | 265 \pm 176 | 1569 \pm 131 | 650 \pm 140 | 2840 \pm 152 | 2741 \pm 228 |

Table 2

Mean \pm standard deviation of the number of micro particles captured by the rotating and stationary SAM2 membranes for non-aggregating (NA), normal aggregating (A) and hyper-aggregating (HA) red blood cells at shear rates of 10 s^{-1} and 2 s^{-1} for a hematocrit of 40% (H40). For comparison, the number of micro particles when using saline in the gap of both concentric cylinders is also given at both shear rates.

| | H40 10 s^{-1} | | H40 2 s^{-1} | |
|----|----------------------------|---------------|---------------------------|---------------|
| | Rotating | Stationary | Rotating | Stationary |
| NA | 353 \pm 103 | 214 \pm 155 | 566 \pm 53 | 244 \pm 200 |
| A | 607 \pm 238 | 300 \pm 179 | 1077 \pm 230 | 604 \pm 100 |
| HA | 1072 \pm 223 | 383 \pm 95 | 1569 \pm 131 | 650 \pm 140 |
| | Saline 10 s^{-1} | | Saline 2 s^{-1} | |
| | 103 \pm 45 | 73 \pm 33 | 80 \pm 32 | 57 \pm 33 |

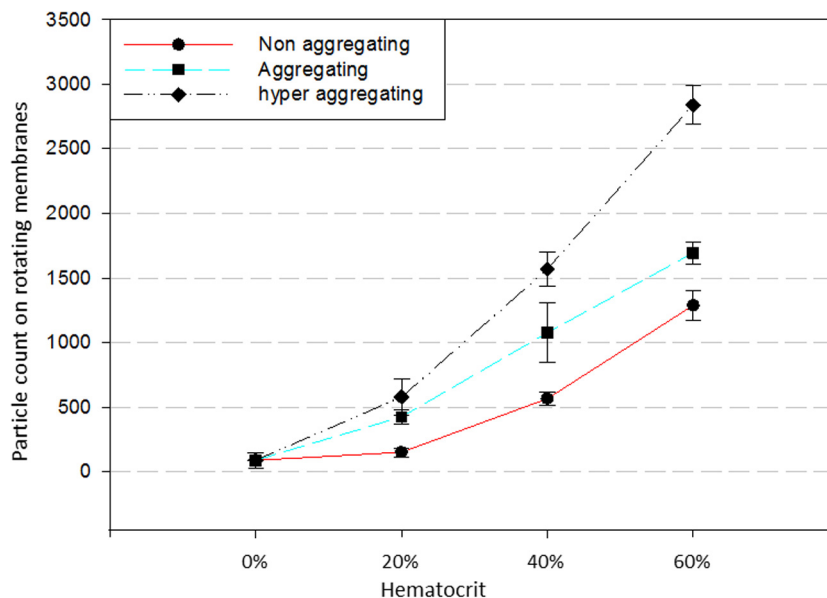


Fig. 3. Mean and standard deviation of the number of micro particles counted on rotating membranes as a function of red blood cell aggregation levels and hematocrits for a constant shear rate of 2 s^{-1} . Statistically significant differences ($p < 0.001$) were found between every hematocrit and blood aggregating level, except for saline versus red blood cells suspended in saline at 20% hematocrit (non-aggregating condition).

As noticed in Figs. 3 and 4, particle margination was enhanced with the level of RBC aggregation. This tendency was observed for every hematocrit and shear rate tested. The results of Fig. 3 also suggest that pathologically high levels of RBC aggregation combined with a high hematocrit would lead to an over concentration of platelets in the near vessel wall region thus further promoting platelet adhesion. These observations are of importance to understand the impact of RBC aggregation on the mechanisms of deep vein thrombosis (Yu et al., 2011). According to a particle exclusion theory (Goldsmith et al., 1999), platelets would be expelled from dense RBC aggregates flowing in the central tubular flow leading to a better lateral migration than in the case of flowing non-aggregating RBCs. This is in accordance with our observations when comparing the impact of RBC saline suspension with no

aggregation (NA) versus normal (N) or hyper-aggregating RBCs (HA). Also, when no interaction could occur in the case of micro particles suspended in saline (i.e., absence of RBCs), minimum adhesions were observed on both Couette walls (Tables 1 and 2), thus sustaining the hypothesis that collision between RBCs and platelets are required for efficient margination.

Chien et al. (1967) observed RBC aggregation to occur at shear rates between 0.0001 s^{-1} and 100 s^{-1} , with more aggregation present at the lowest range. In conditions such as diabetes mellitus, shear rates above 100 s^{-1} might be necessary to disrupt RBC pathological aggregates (Cloutier et al., 2008). This range of shear rates is relevant for venous flow thrombogenicity but also applies to arterial or cardiac recirculating flow (see for example the phenomenon of spontaneous echo contrast within heart cavities known to be a

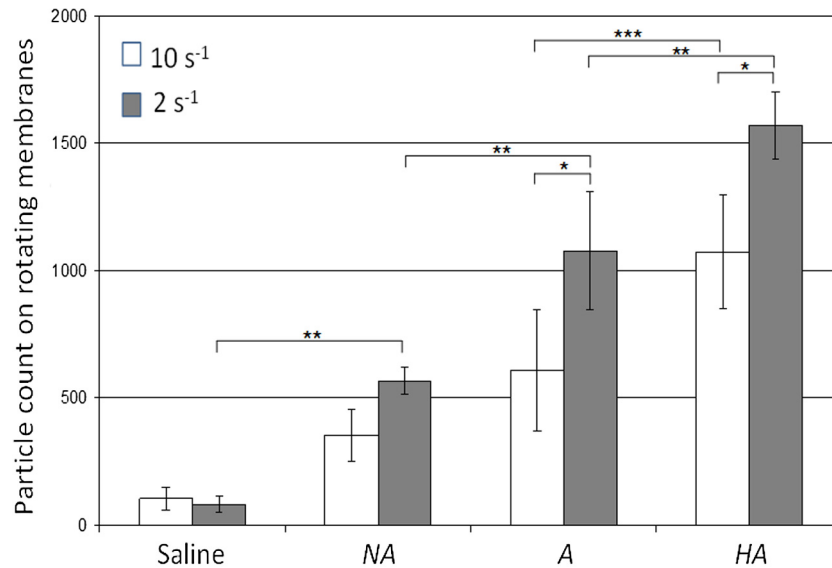


Fig. 4. Mean and standard deviation of the number of micro particles counted on rotating membranes as a function of the RBC aggregation level (no aggregation – NA, normal aggregation – A, hyper-aggregation – HA) at two shear rates and a constant hematocrit of 40% (* shear rate pairwise difference with $p < 0.001$; ** suspending micro particle solution pairwise difference at 2 s^{-1} with $p < 0.001$; *** suspending micro particle solution pairwise difference at 10 s^{-1} with $p < 0.001$). Results for the saline suspensions are given as controls.

risk factor of thrombotic events and attributed to recirculating or stagnant RBC aggregates (Beppu et al., 1985; Daniel et al., 1988; Wang et al., 1992; Black, 2000)).

As noticed experimentally, the micro particle adhesion was enhanced with the hematocrit, which was varied from 0% to 60% in our study. This is in line with the results of Yeh and Eckstein (1994) observing faster platelet-sized particle migration velocity in flowing blood when the hematocrit was greater than 10%. This also supports pioneered observation that anemic patients have a longer bleeding time than control individuals (Hellem et al., 1961). As routinely experienced in critical care medicine, the bleeding time returns to normal if the hematocrit is raised above 30% by blood transfusion.

4.1. Rotating versus static biotin-capturing membrane

As noticed in Tables 1 and 2, more particles were captured by the rotating inner cylinder and this remained true in the absence of RBCs, circulating non-aggregating RBCs or flowing RBCs with different aggregation levels. Experimental observations supported by rheological modeling have been made for spheres suspended in a Newtonian fluid at high volume concentrations and sheared in Couette flow (corresponding to our experiments in the absence of RBCs but at a lower volume concentration of micro particles) (Leighton and Acrivos, 1987). Two particle diffusion processes with different time scale of a few seconds or a few hours were observed. In both cases, modeling suggested that these observations were due to particle interactions and migration leading to gradients in particle concentration within the gap of the Couette system. Magnetic resonance microscopy confirmed the radial migration of particles from the rotating inner cylinder toward the static outer cylinder (Chow et al., 1994). Similar observations were made with RBCs at a normal hematocrit (Cokelet et al., 2005). Since more micro particles were detected in our study on the moving inner cylinder, one cannot exclude the impact of the micro particle injection toward this cylinder (see Fig. 1). However, even if this confounding effect could exist, we observed more micro particle fixation on biotin membranes for both inner and outer walls when they were interacting with non-aggregating or aggregating RBCs, thus confirming the validity of our rheological observations.

In the current study, the use of a Couette system allowed fundamental observations at predetermined constant shear rates. It is clear that blunt-to-parabolic flow streamlines in tube-like flow should enhance the complexity of micro particle interactions, margination and segregation. Flow pulsatility, vessel caliber, vessel tapering and the cardiovascular system geometry further complicate cellular interactions. Recent developments in microfluidics are also underrepresenting the complexity of blood cell interactions (Kumar and Graham, 2012; Mehri et al., 2014). Nevertheless, observations with these different systems are complementary and very useful to clarify the role of RBCs (and their aggregates) on micro particle rheology.

4.2. Implications for molecular imaging and drug delivery

To adhere to vessel walls or specific molecular sites, targeted micro and nano particles must circulate at the vicinity of the vascular wall in the same manner as the micro particles of this study. For arterial applications, flow hemodynamics and blood hematocrit dominate the margination process. However, RBC aggregation is relevant to the context of molecular imaging of the venous system using injected targeted micro particles (Unger et al., 2000; Katoh et al., 2009). RBC aggregation may also be of high relevance for drug delivery in the microcirculation, although this phenomenon has not yet been specifically considered (Tan et al., 2012; Müller et al., 2014; D'Apolito et al., 2015). Note that the biotin streptavidin adhesion privileged in this study is similar to that used for drug delivery using targeted micro particles. Blood rheology and RBC aggregation are finally of importance in the context of deoxyribonucleic acid delivery for genetic therapy (Hernot and Klibanov, 2008).

5. Conclusion

In this study, an experimental Couette flow device was used to confirm the impact of blood hematocrit on micro particle margination, and to quantify the amount of fluorescent labeled particles attaching to the wall under conditions promoting RBC aggregation (i.e., a low shear rate and presence of plasma or dextran micro-molecules favoring RBC adhesion). The phenomenon of RBC aggrega-

gation was observed at shear rate conditions mimicking venous flow, recirculating flow or plug flow. The 2-mm gap of the Couette flow device corresponds to the diameter of a small vein. The conclusions of this study may apply to microcirculatory flow but further validation would be required. The direct impact of this work is the better understanding of the role of RBC aggregation on venous thrombosis, and the potential impact of RBC clustering on diffusion efficacy of micro particle imaging contrasts and drug carriers toward the vessel wall.

Conflict of interest

Authors have no conflict of interest to declare.

Acknowledgments

This work was supported by the Canadian Institutes of Health Research (grant #MOP-84358).

References

- Aarts, P.A., Bolhuis, P.A., Sakariassen, K.S., Heethaar, R.M., Sixma, J.J., 1983. Red blood cell size is important for adherence of blood platelets to artery subendothelium. *Blood* 62, 214–217.
- Aarts, P.A., Heethaar, R.M., Sixma, J.J., 1984. Red blood cell deformability influences platelets – vessel wall interaction in flowing blood. *Blood* 64, 1228–1233.
- Aarts, P.A., van den Broek, S.A., Prins, G.W., Kuiken, G.D., Sixma, J.J., Heethaar, R.M., 1988. Blood platelets are concentrated near the wall and red blood cells, in the center in flowing blood. *Arterioscler. Thromb. Vasc. Biol.* 8, 819–824.
- Almomani, T., Udaykumar, H.S., Marshall, J.S., Chandran, K.B., 2008. Micro-scale dynamic simulation of erythrocyte – platelet interaction in blood flow. *Ann. Biomed. Eng.* 36, 905–920.
- Amersham Biosciences, 2008. *ImageQuant TL User Guide*.
- Barthes-Biesel, D., Sgaier, H., 1985. Role of membrane viscosity in the orientation and deformation of a spherical capsule suspended in shear flow. *J. Fluid Mech.* 160, 119–135.
- Ben Ami, R., Barshtein, G., Zeltser, D., Goldberg, Y., Shapira, I., Roth, A., Keren, G., Miller, H., Prochorov, V., Eldor, A., Berliner, S., Yedgar, S., 2001. Parameters of red blood cell aggregation as correlates of the inflammatory state. *Am. J. Physiol. (Heart Circulatory Physiol.)* 280, H1982–H1988.
- Beppu, S., Nimura, Y., Sakakibara, H., Nagata, S., Park, Y.D., Izumi, S., Ueoka, M., Masuda, Y., Nakasone, I., 1985. Smoke-like echo in the left atrial cavity in mitral valve disease: its features and significance. *J. Am. Coll. Cardiol.* 6, 744–749.
- Berliner, S., Rogowski, O., Aharonov, S., Mardi, T., Tolshinsky, T., Rozenblat, M., Justo, D., Deutsch, V., Serov, J., Shapira, I., Zeltser, D., 2005. Erythrocyte adhesiveness/aggregation: a novel biomarker for the detection of low-grade internal inflammation in individuals with atherothrombotic risk factors and proven vascular disease. *Am. Heart J.* 149, 260–267.
- Black, I.W., 2000. Spontaneous echo contrast: where there's smoke there's fire (review). *Echocardiography* 17, 373–382.
- Boynard, M., Lelievre, J.C., 1990. Size determination of red blood cell aggregates induced by dextran using ultrasound backscattering phenomenon. *Biorheology* 27, 39–46.
- Cadroy, Y., Hanson, S.R., 1990. Effects of red blood cell concentration on hemostasis and thrombus formation in a primate model. *Blood* 75, 2185–2193.
- Chien, S., 1975. Biophysical behavior of red cells in suspensions. In: Surgenor, D.M. (Ed.), *The Red Blood Cell*. Academic Press, New York, San Francisco, London, pp. 1031–1133.
- Chien, S., Usami, S., Dellenback, R.J., Gregerson, M.I., Nanninga, N.B., Guest, M., 1967. Blood viscosity: influence of erythrocyte aggregation. *Science* 157, 829–831.
- Chow, A.W., Sinton, S.W., Iwamiya, J.H., Stephens, T.S., 1994. Shear induced particle migration in Couette and parallel-plate viscometers: NMR imaging and stress measurements. *Phys. Fluids* 6, 2561–2576.
- Cloutier, G., Zimmer, A., Yu, F.T.H., Chiasson, J.L., 2008. Increased shear rate resistance and fastest kinetics of erythrocyte aggregation in diabetes measured with ultrasound. *Diabetes Care* 31, 1400–1402.
- Cokelet, G.R., Brown, J.R., Codd, S.L., Seymour, J.D., 2005. Magnetic resonance microscopy determined velocity and hematocrit distributions in a Couette viscometer. *Biorheology* 42, 385–399.
- D'Apolito, R., Tarabali, F., Minardi, S., Liu, X., Caserta, S., Cevenini, A., Tasciotti, E., Tomaiuolo, G., Guido, S., 2016. Microfluidic interactions between red blood cells and drug carriers by image analysis techniques. *Med. Eng. Phys.* 38, 17–23.
- D'Apolito, R., Tomaiuolo, G., Tarabali, F., Minardi, S., Kirui, D., Lui, X., Cevenini, A., Palomba, R., Ferrari, M., Salvatore, F., Tasciotti, E., Guido, S., 2015. Red blood cells affect the margination of microparticles in synthetic microcapillaries and intravital microcirculation as a function of their size and shape. *J. Control. Release* 217, 263–272.
- Daniel, W.G., Nellessen, U., Schröder, E., Nonnast-Daniel, B., Bednarski, P., Nikutta, P., Lichtlen, P.R., 1988. Left atrial spontaneous echo contrast in mitral valve disease: an indicator for an increased thromboembolic risk. *J. Am. Coll. Cardiol.* 11, 1204–1211.
- Eckstein, E.C., Tilles, A.W., Millero, F.J., 1988. Conditions for the occurrence of large near-wall excesses of small particles during blood flow. *Microvasc. Res.* 36, 31–39.
- Eugster, M., Reinhart, W.H., 2005. The influence of the haematocrit on primary haemostasis in vitro. *Thromb. Haemost.* 94, 1213–1218.
- Fung, Y.C., 1997. *Biomechanics: Circulation*. Springer, New York, Berlin, Heidelberg.
- Goldsmith, H.L., 1972. The flow of model particles and blood cells and its relation to thrombogenesis. *Prog. Hemost. Thromb.* 1, 97–127.
- Goldsmith, H.L., 1993. Poiseuille medal award lecture: from papermaking fibers to human blood cells. *Biorheology* 30, 165–190.
- Goldsmith, H.L., Bell, D.N., Spain, S., McIntosh, F.A., 1999. Effect of red blood cells and their aggregates on platelets and white cells in flowing blood. *Biorheology* 36, 461–468.
- Goldsmith, H.L., Marlow, J.C., 1979. Flow behavior of erythrocytes. II. Particle motions in concentrated suspensions of ghost cells. *J. Colloid Interface Sci.* 71, 383–407.
- Goldsmith, H.L., Turitto, V.T., 1986. Rheological aspects of thrombosis and haemostasis: basic principles and applications. *Thromb. Haemost.* 55, 415–435.
- Hellem, A.J., Borchgrevink, C., Ames, S.B., 1961. The role of red cells in haemostasis: the relation between haematocrit, bleeding time and platelet adhesiveness. *Br. J. Haematol.* 7, 42–50.
- Hernot, S., Klibanov, A.L., 2008. Microbubbles in ultrasound-triggered drug and gene delivery. *Adv. Drug Deliv. Rev.* 60, 1153–1166.
- Jain, A., Munn, L.L., 2009. Determinants of leukocyte margination in rectangular microchannels. *PLoS ONE* 4, e7104(1)–e7104(8).
- Johnson, V.E., 2013. Revised standards for statistical evidence. *Proc. Natl. Acad. Sci. USA* 110, 19313–19317.
- Katoh, M., Haage, P., Wiethoff, A.J., Günther, R.W., Bücker, A., Tacke, J., Spuentrup, E., 2009. Molecular magnetic resonance imaging of deep vein thrombosis using a fibrin-targeted contrast agent: a feasibility study. *Invest. Radiol.* 44, 146–150.
- Keller, K.H., 1971. Effect of fluid shear on mass transport in flowing blood. *Federation Proc.* 30, 1591–1599.
- Keller, S.R., Skalak, R., 1982. Motion of a tank-treading ellipsoidal particle in a shear flow. *J. Fluid Mech.* 120, 27–47.
- Kumar, A., Graham, M.D., 2012. Margination and segregation in confined flows of blood and other multicomponent suspensions. *Soft Matter* 8, 10536–10548.
- Leighton, D., Acrivos, A., 1987. The shear-induced migration of particles in concentrated suspensions. *J. Fluid Mech.* 181, 415–439.
- Litvinov, R.I., Weisel, J.W., 2017. Role of red blood cells in haemostasis and thrombosis. *Int. Soc. Blood Transfus. Sci. Ser.* 12 (1), 176–183.
- Mackman, N., 2012. New insights into the mechanisms of venous thrombosis. *J. Clin. Invest.* 122, 2331–2336.
- Maharskak, N., Arbel, Y., Shapira, I., Berliner, S., Ben-Ami, R., Yedgar, S., Barshtein, G., Dotan, I., 2009. Increased strength of erythrocyte aggregates in blood of patients with inflammatory bowel disease. *Inflamm. Bowel Dis.* 15, 707–713.
- McNamara, P., Lew, W., Han, L., 2001. Fluorescent imaging and analysis with Typhoon 8600. *Electrophoresis* 22, 837–842.
- Mehri, R., Mavriplis, C., Fenech, M., 2014. Design of a microfluidic system for red blood cell aggregation investigation. *J. Biomech. Eng.* 136, 064501(1)–064501(5).
- Müller, K., Fedosov, S.A., Gompper, G., 2014. Margination of micro- and nanoparticles in blood flow and its effect on drug delivery. *Sci. Rep.* 4, 4871(1)–4871(8).
- Nash, G.B., Watts, T., Thornton, C., Barigou, M., 2008. Red cell aggregation as a factor influencing margination and adhesion of leukocytes and platelets. *Clin. Hemorheol. Microcirculat.* 39, 303–310.
- Neu, B., Meiselman, H.J., 2002. Depletion-mediated red blood cell aggregation in polymer solutions. *Biophys. J.* 83, 2482–2490.
- Pearson, M.J., Lipowsky, H.H., 2000. Influence of erythrocyte aggregation on leukocyte margination in postcapillary venules of rat mesentery. *Am. J. Physiol. (Heart Circulatory Physiol.)* 279, H1460–H1471.
- Promega, 2008. *SAM2 Biotin Capture Membrane, Instructions for use of Products*.
- Reasor, D.A., Mehrabadi, M., Ku, D.N., Aidun, C.K., 2013. Determination of critical parameters in platelet margination. *Ann. Biomed. Eng.* 41, 238–249.
- Reggiori, G., Occhipinti, G., De Gasperi, A., Vincent, J.L., Piagnerelli, M., 2009. Early alterations of red blood cell rheology in critically ill patients. *Crit. Care Med.* 37, 3041–3046.
- Savage, B., McFadden, P.R., Hanson, S.R., Harker, L.A., 1986. The relation of platelet density to platelet age: survival of low- and high-density 111 indium-labeled platelets in baboons. *Blood* 68, 386–393.
- Schaefer, E.M., Guimond, S., 1998. Detection of protein tyrosine kinase activity using a high-capacity streptavidin-coated membrane and optimized biotinylated peptide substrates. *Anal. Biochem.* 261, 100–112.
- Schneider, D.J., Tracy, P.B., Mann, K.G., Sobel, B.E., 1997. Differential effects of anticoagulants on the activation of platelets ex vivo. *Circulation* 96, 2877–2883.
- Tan, J., Thomas, A., Liu, Y., 2012. Influence of red blood cells on nanoparticle targeted delivery in microcirculation. *Soft Matter* 8, 1934–1946.
- Tripetto, J., Denault, A.Y., Allard, L., Chayer, B., Perreault, L.P., Cloutier, G., 2013. Ultrasound monitoring of RBC aggregation as a real-time marker of the inflammatory response in a cardiopulmonary bypass swine model. *Crit. Care Med.* 41, e171–e178.
- Turitto, V.T., Hall, C.L., 1998. Mechanical factors affecting hemostasis and thrombosis. *Thromb. Res.* 92, S25–S31.

- Unger, E., Metzger, P., Krupinski, E., Baker, M., Hulett, R., Gabaeff, D., Mills, J., Ihnat, D., McCreery, T., 2000. The use of a thrombus-specific ultrasound contrast agent to detect thrombus in arteriovenous fistulae. *Invest. Radiol.* 35, 86–89.
- Vahidkhah, K., Bagchi, P., 2015. Microparticle shape effects on margination, nearwall dynamics and adhesion in a three-dimensional simulation of red blood cell suspension. *Soft Matter* 11, 2097–2109.
- Wang, X.F., Liu, L., Cheng, T.O., Li, Z.A., Deng, Y.B., Wang, J.E., 1992. The relationship between intracardiovascular smoke-like echo and erythrocyte rouleaux formation. *Am. Heart J.* 124, 961–965.
- Weng, X., Cloutier, G., Beaulieu, R., Roederer, G.O., 1996a. Influence of acute-phase proteins on erythrocyte aggregation. *Am. J. Physiol.* 271, H2346–H2352.
- Weng, X., Cloutier, G., Pibarot, P., Durand, L.G., 1996b. Comparison and simulation of different levels of erythrocyte aggregation with pig, horse, sheep, calf, and normal human blood. *Biorheology* 33, 365–377.
- Weng, X., Roederer, G.O., Beaulieu, R., Cloutier, G., 1998. Contribution of acute-phase proteins and cardiovascular risk factors to erythrocyte aggregation in normolipidemic and hyperlipidemic individuals. *Thromb. Haemost.* 80, 903–908.
- Whorlow, R.W., 1980. *Rheological Techniques*. Ellis Horwood, Chichester.
- Woldhuis, B., Tangelder, G.J., Slaaf, D.W., Reneman, R.S., 1993. Influence of dextrans on platelet distribution in arterioles and venules. *Eur. J. Physiol.* 425, 191–198.
- Yeh, C., Eckstein, E.C., 1994. Transient lateral transport of platelet-sized particles in flowing blood suspensions. *Biophys. J.* 66, 1706–1716.
- Yu, F.T.H., Armstrong, J., Tripette, J., Meiselman, H.J., Cloutier, G., 2011. A local increase in red blood cell aggregation can trigger deep vein thrombosis: evidence based on quantitative cellular ultrasound imaging. *J. Thromb. Haemost.* 9, 481–488.
- Yu, F.T.H., Franceschini, E., Chayer, B., Armstrong, J., Meiselman, H.J., Cloutier, G., 2009. Ultrasonic parametric imaging of erythrocyte aggregation using the structure factor size estimator. *Biorheology* 46, 343–363.
- Zhao, H., Shaqfeh, E.S.G., Narsimhan, V., 2012. Shear-induced particle migration and margination in a cellular suspension. *Phys. Fluids* 24, 011902-1–011902-21.